International Journal of Research in Advent Technology, Special Issue, August 2018
E-ISSN: 2321-9637
International Conference on "Topical Transcends in Science, Technology and Management" (ICTTSTM-2018)
Available online at www.ijrat.org

Nio Nanoparticles and Its Antibacterial Activity

R.S. RAVEENDRA[A, B], P.A. PRASHANTH[C*], S. SATHYANARAYANI[A], B.M. NAGABHUSHANA[D]
[a]*Department of Chemistry, Sai Vidya Institute of Technology, Bangalore- 560 064, India*
[b]*Research and Development Centre, Bharathiar University, Coimbatore -641 046, India*
[c]*Department of Chemistry,PES College of Engineering, Mandya-571 401, India*
[d]Department of Chemistry, M.S. Ramaiah Institute of Technology, Bangalore- 560 054, India

ABSTRACT

In the current work we focused on the antibacterial activity of NiO nanoparticles prepared using glycine as a fuel in combustion route. The synthesized product was characterized by powder X-ray diffraction, field emission scanning electron microscopy, high resolution transmission emission microscopy, energy-dispersive X-ray spectroscopy, Fourier transformer infra red spectroscopy and Brunauer–Emmett–Teller (BET) surface area measurement. Antibacterial studies were examined against gram -ve *Escherichia coli,* and gram +ve *Staphylococcus aureus* bacteria's by agar well diffusion method. The NiO nanoparticles showed substantial effect on both the bacterial strains. The results indicate that NiO nanoparticles could potentiate the permeability of bacterial cell wall and remarkably increases antibacterial activity thereby facilitate the synergistic impact on growth inhibition of bacterial strains.

Keywords— staphylococcus aureus; antibacterial; solution combustion; NiO nanoparticles

INTRODUCTION

In the current science technology fields, nanostructured particles show new properties owing to their very small size that are significantly different from those of their bulk equivalents. Many researchers of material sciences have already been examined the transition metal oxide nanoparticles and their unique characteristics. These transition metal oxide nanoparticles are gaining constant significance for various applications such as antibacterial, catalysis, dye adsorption, passive electronic components and ceramic materials [1].

Due to uniform size and well dispersal capacity, NiO nanoparticles are more attractive towards various applications such as magnetic, ceramic, biological and heterogeneous catalysis [2]. Different methods have been already used to synthesize NiO nanoparticles, few methods are sol–gel [3], surfactant-mediated synthesis [4] thermal decomposition [5], polymer-matrix assisted synthesis [6] and spray-pyrolysis [7]. In addition to these, well known common methods such as hydrothermal synthesis, pyrolysis by microwave, precipitation-calcination, ultrasonic radiation, carbonyl method, laser chemical method, micro emulsion method and combustion are also have been used [8-13]. However, to the best of our knowledge, most of the reported experimental techniques for the synthesis of nanopowders are still limited in laboratory scale due to some unresolved problems, such as special conditions, tedious processes, complex apparatus, low yield and high cost [14].

In recent years, the improvement of antibacterial agents with no negative effects or little impact on the natural environment is of particular importance in nanotechnology. Industrial effluents are exposed to contamination with microorganisms and organic compounds. Therefore, water purification requires a major technology in the biochemical and biological industries [15].

In the current article, we are presenting the synthesis and characterization of NiO nanoparticles by simple solution combustion method using glycine as fuel. We studied the antibacterial activity of NiO nanoparticles against gram negative and gram positive bacteria.

EXPERIMENTAL

Materials and methods:

Analytically graded chemicals and reagents were used in this work. Nickel nitrate ($Ni(NO_3)_2$ $6H_2O$, 99% Merck), Glycine ($C_2H_5NO_2$ 99 % Merck), Ciprofloxacin were used without any further purification.

Synthesis of NiO nanoparticles:

The NiO nanoparticles was prepared by simple solution combustion synthesis method [16, 17] using ($Ni(NO_3)_2$ $6H_2O$, and $C_2H_5NO_2$ as oxidizer and fuels respectively, First precursor mixture was stirred well using magnetic stirrer for about 15 min with double distilled water. Then the combustion process was carried out in a pre-heated muffle furnace at 500 ±10 °C. Initially the entire solution boils, resulted viscous liquid catches fire, auto ignited with flames on surface forming a green powdered product.

Characterization techniques:

The confirmation for the formation of NiO nanoparticles and crystallite size was studied by PXRD recorded on a Shimadzu XRD-700 X-ray Diffractometer with CuKα radiation with diffraction angle range 2θ = 30˚ to 80˚ operating at 40 kV and 30 mA. To study the morphology of the product, FE-SEM was performed on a ZEISS ULTRA 55 scanning electron microscope. High-resolution transmission electron microscope (HR-TEM, 2010F). Selected area electron diffraction (SAED) was carried on a Hitachi H-8100 (accelerating voltage upto 200 KV, LaB_6 Filament). The FT-IR studies have been recorded on a Perkin Elmer Spectrometer (Spectrum 1000) with KBr pellet method in the range of 500-4000 cm^{-1} The total surface area of the synthesized NiO nanoparticles was measured using nitrogen adsorption/desorption isotherms with a Brunauer-Emmett- Teller (BET) surface area analyzer (ASAP 2020) at the bath temperature -196.329 ºC.

RESULT AND DISCUSSIONS

PXRD studies and crystallite size:

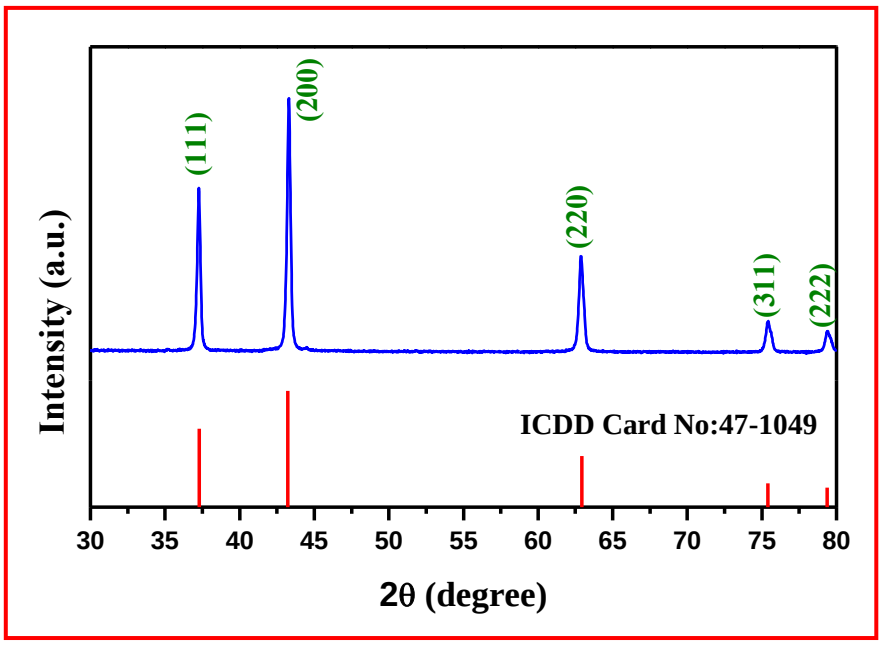

Fig.1 PXRD patterns of NiO nanoparticles

The PXRD of the sample showed the crystalline nature having cubic structure (matched with ICDD card number 89-7130 with space group Fm-3m (No-225)), and cell parameters a = b= c =4.1771 Å. All the diffraction peaks can be indexed to (1 1 1), (2 0 0), (2 2 0), (3 1 1) and (2 2 2) reflections. The inherent nature of nanocrystals can clearly indicated by broadening of the reflections. Fig.1 shows the powder X-ray diffraction patterns of NiO nanoparticles. The crystallite size is calculated from the full width at half maximum (FWHM (β)) of the diffraction peaks using Debye- Scherer's method [18] using the following equation,

$$d = \frac{k\lambda}{\beta \cos \theta} \quad \text{---------- (1)}$$

'd' is the average crystalline dimension perpendicular to the reflecting phases, 'λ' is the X-ray wavelength, 'k' is Scherer's constant (0.92), 'β' is the full width at half maximum (FWHM) intensity of a Bragg reflection excluding instrumental broadening and 'θ' is the Bragg's angle (30˚- 80˚). The calculated average crystallite size of the product is found in the range of 20-25 nm. The packing diagram of the NiO nanoparticles obtained using diamond software is shown in Fig. 2 and all the lattice and the structural parameters are presented in the Table-1.

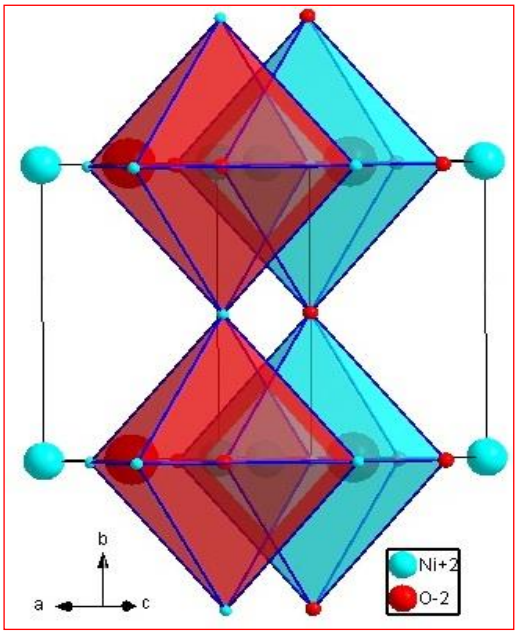

Fig. 2 Crystal structure of NiO nanoparticles

Atoms	Oxidation state	Wyckoff notation	x/a	y/b	z/c	Occupancy
Ni	2+	4c	0.0000	0.0000	0.3580	1
O	2-	4b	0.5000	0.5000	0.5000	1
Crystal system: Cubic; Lattice: Face Centered: space group: Fm-3m (225); ICDD: 47-1049						

Table-1 Crystal lattice and structural parameters

FT-IR spectroscopic studies:

Fourier Transform Infrared (FTIR) spectroscopy is used to get valuable insight into the functional groups of a particular system. It is owing to molecular vibrational excitation energy is in the range of 1013 – 1014 Hz, which corresponds to infrared radiation. This means that FTIR spectroscopy is ideal for observing the vibrational transitions of self-assembled functional groups coordinated to nanoparticle surfaces, and both qualitative and quantitative analysis are possible [19].

Fig. 3 shows FT-IR spectrum of the NiO nanoparticles taken to describe the vibrational frequency of Ni–O and other bonds related to impurities present in the NiO nanoparticles. There are no impurity peaks corresponding to the organic matter in the sample. Strong absorption bands at 695 cm^{-1} can be assigned to the stretching vibration of Ni–O bond [20].

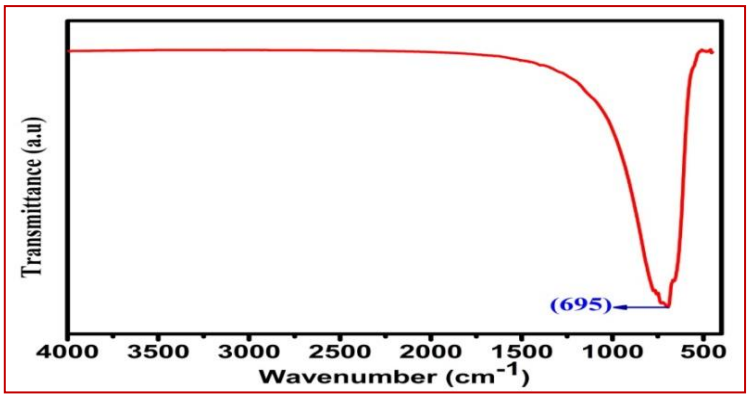

Fig.3 FTIR spectrum of NiO nanoparticles

Morphological analysis:

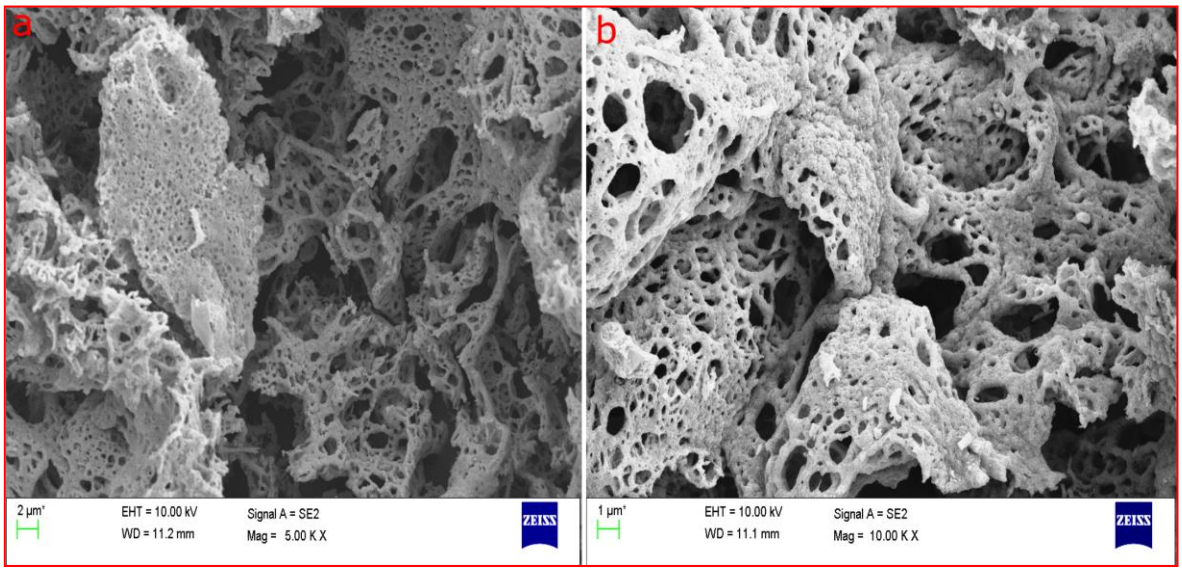

Fig. 4(a, b) FE-SEM NiO nanoparticles at different magnifications

The morphology of prepared NiO nanoparticles was obtained using field emission scanning electron microscopy (FE-SEM). Fig. 4(a, b) shows FE-SEM images NiO nanoparticles at different magnifications. It reveals that the morphology of the NiO nanoparticles is a porous and has net like structure. The confirmation for the crystallinity was examined by TEM images. This method is superior to PXRD, that it is direct and less likely to be affected by experimental errors and or other properties of the particles. TEM images of NiO nanoparticles (Fig. 5a) shows that the particles obtained are in nano regime and have highly crystalline and average particle size ~100 m. Various SAED patterns were obtained from the NiO nanoparticles. These patterns and the tilting angles matched well with the cubic NiO crystal as shown in Fig. 5(b).

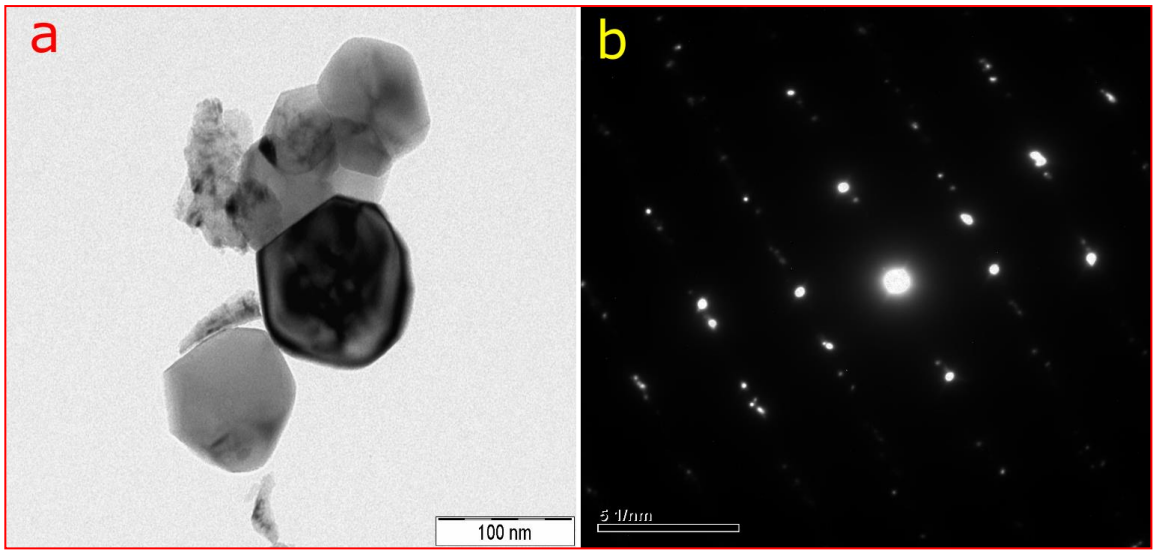

Fig. 5(a) TEM and (b) SAED patterns of NiO nanoparticles

BET surface area analysis:

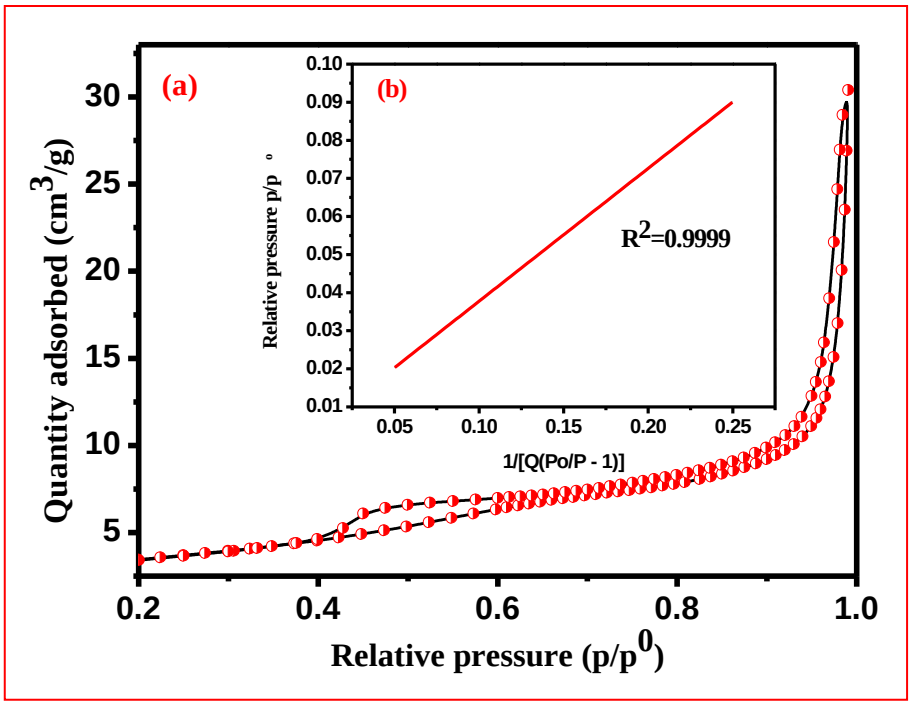

Fig. 6(a) Nitrogen adsorption/desorption isotherms of NiO nanoparticles at -196.329 ºC (b) BET surface area linear plot

Total surface area of the sample was calculated with the help of Brunauer–Emmett–Teller (BET) multi-point and single-point methods using the N_2 adsorption isotherm data [21]. Before analysis, all of the obtained NiO nanoparticles were evacuated under vacuum condition at 150 ºC overnight in order to clean all the pores. The pore volume data were calculated by using BJH method which is the procedure for calculating pore size distribution using the Kelvin equation and DH methods. The micropore volumes of the samples were obtained using Dubinin–Radushkevich (DR) method [22]. The pore size distribution was determined by using the BJH model. All experimental parameters of BET surface area analysis are summarized in the Table-2. Fig. 6 (a-b) shows the N_2 adsorption/desorption isotherms and BET surface area plot of NiO nanoparticles.

surface area	Pore volume	Pore size	Micro pore s. area	BJH Adsorption average pore diameter	BJH Desorption average pore diameter	D-H Adsorption average pore diameter	D-H Desorption average pore diameter
12.4 m^2/g	0.05 cm^3/g	15.2 nm	10.7 m^2/g	17.7 nm	13.8 nm	16.1 nm	14.1 nm

Table-2 BET surface area parameters

Bactericidal activity studies:

The antibacterial activity of the synthesized NiO nanoparticles against gram negative *Escherichia coli* NCIM-5051 and gram positive *Staphylococcus aureus* NCIM-5022 bacteria's were examined using agar well diffusion technique [23-25]. For growing bacterial culture Muller hinton agar was used and nutrient agar plates were prepared and swabbed using sterile L-shaped glass rod with 100 µl of 24 h mature broth culture of individual bacterial strains. The wells were made by using sterile cork borer (6mm) and were created into the each petri-plate. Varied concentrations of NiO nanoparticles (500 and 1000 µg/well) were used to assess the activity. Compound was dispersed in sterile water and it was used as a negative control and simultaneously the standard antibiotic *Ciprofloxacin* (5µg/50µl) (Hi Media, Mumbai, India) as positive control were tested against the bacterial pathogens. Then the plates were incubated at 37 °C for 24 – 36 h, the zone of inhibition measured

in millimeter of the every well and also the values were noted. Triplicates were maintained in every concentration and also the average values were calculated for the ultimate antibacterial activity.

The results show that the negative control, DMSO did not show any inhibition zone, which means that the control alone without nanoparticles does not show any antibacterial activity. When the loading of NiO nanoparticles was 500 mg, the inhibition of gram negative *Escherichia coli* is better than the gram positive *Staphylococcus aureus*. However, when the load of NiO nanoparticles was increased to 1000 mg, no significant difference in the inhibition zone was observed among both the bacteria's. The nanoparticles showed highest inhibition activity on the only gram negative studied. The zone of inhibition observed for this bacterial strain was 3.9 mm, Further, the statistical error was evaluated using ez Anova statistical software and the P value was found to be <0.05 indicating that the error is well within the limit. The zone of inhibition is given in Fig. 7(a, b) and data are given in Table-3 and represented in histograph (Fig. 8.)

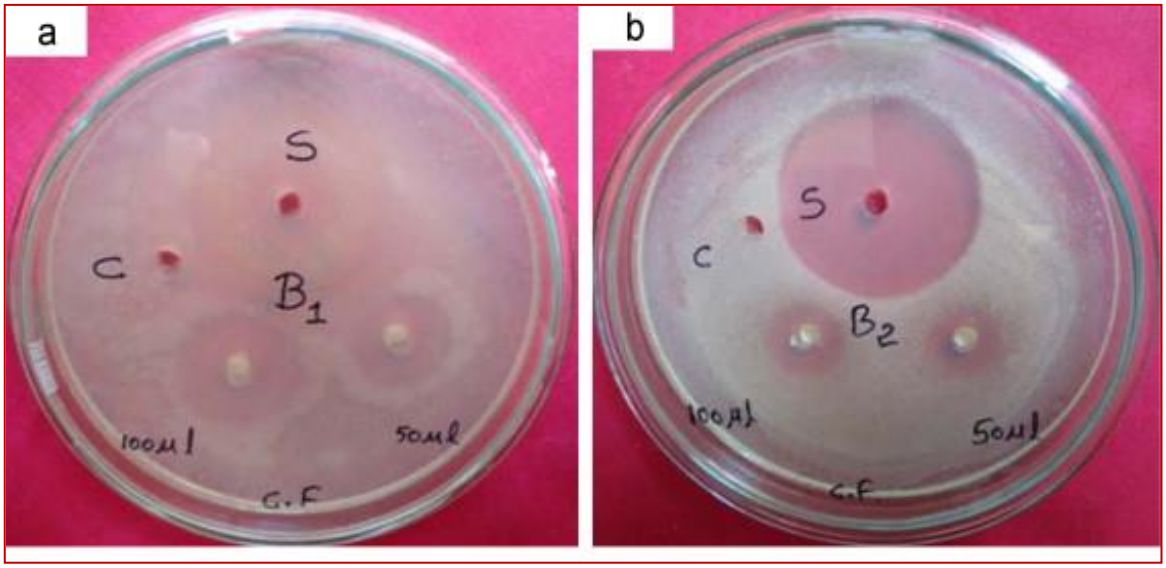

Fig. 7(a, b) Zone of inhibition tests for NiO nanoparticles against *E. Coli* and *S. Aureus*

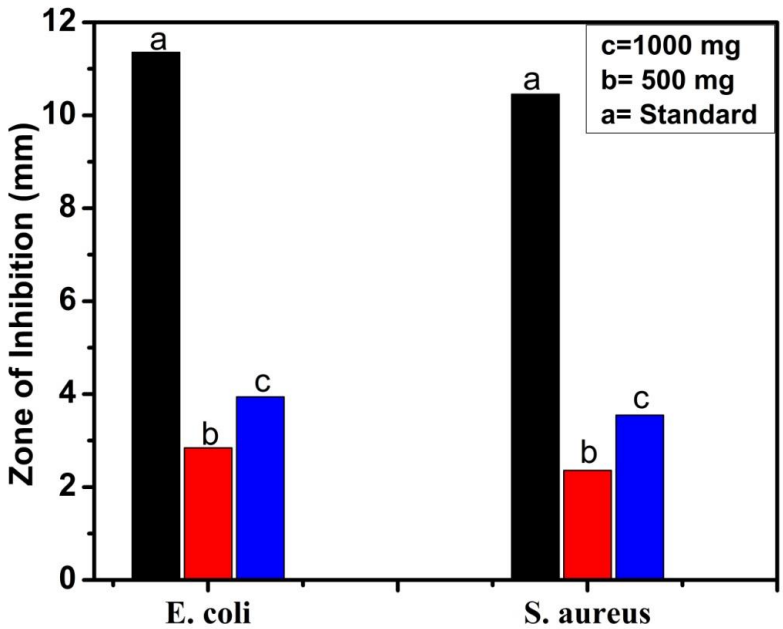

Fig. 8 Histograph showing comparison of antibacterial activity of *E. Coli* and *S. Aureus*

Sl. No	Treatment	*Escherichia coli* (Mean±SE)	*Staphyloccus aureus* (Mean±SE)
I	Standard (5µg/50µL)	11.00±0.41	10.45±0.25
II	NiO (500mg)	2.84±0.24	2.35±0.14
III	NiO (1000mg)	3.00±0.38	2.54±0.48

Table-3 Bactericidal activity of NiO nanoparticles on pathogenic bacterial strains

Mechanism of antibacterial activity:

The fallowing factor may be responsible antibacterial activity viz (i) the cationic size of NiO nanoparticles and (ii) reactive oxygen species (ROS) formation [26]. The antibacterial effect of these NiO nanoparticles seems to be administered by the presence of ionic and colossal structural patterns which is in good agreement with the pharmacophore. The presence of these helps the compounds to interact or penetrate more with cell membrane of the bacteria's and there by inactivating them. This may be due to the distance between the positively charged groups and the nanoparticles. Another widely postulated mechanism is that of the "*self-promoted uptake*" [27] of the antibiotic across the outer membranes of bacteria which consist of lipopolysaccaride surface. This suggests that the nanoparticles interact with the charged outer membrane and subsequent channel formation in the cytoplasmic membrane via either "*Barrel-Stave*" or "*Carpet*" mechanism [28, 29] resulting in cell death. Fig. 9 explains the pictorial mechanism of antibacterial activity.

The mechanism of antibacterial activity can also be explained based on surface area measurements. The fact that small nanoparticles tend to be more toxic than large nanoparticles can be explained by the small NPs relative larger surface area to volume ratio as compared to larger nanoparticles. This can greatly increase the production of ROS is greatly increased (see below), which consequently can damage and inactivate essential biomolecules, including DNA, proteins, and lipids [30].

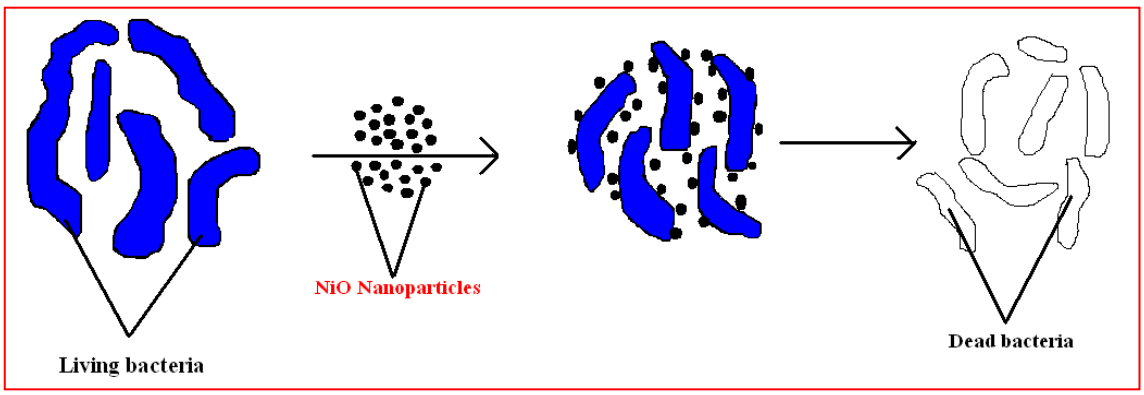

Fig. 9 Possible mechanisms of antibacterial activity NiO nanoparticles

CONCLUSIONS

The NiO nanoparticles were successfully synthesized by simple solution combustion synthesis method and studied its characteristics by various electro analytical techniques. Antibacterial activity of the NiO nanoparticles was evaluated with 2 different bacterial pathogens. Results of bactericidal tests concludes that at slightly higher concentration (500 mg) of NiO nanoparticles can acts as an good antibacterial agent against gram negative *Escherichia coli* and gram positive *Staphylococcus aureus* bacteria in agar well diffusion method.

REFERENCES

[1]. K.C. Patil, S.T. Aruna and S. Ekambaran, Curr. Opp. Solid State Mater. Sci. 2:158, (1997)
[2]. M. L. Peterson, A. F. White, G.E. Brown, G.A. Jr Parks, Environmental Sci. Technol. 31:1573, (1997)

[3]. C.N. R. Rao, Chemical applications of infrared spectroscopy. (New York & London: Academic Press) (1963)
[4]. C.N. R. Rao. Chemical approaches to the Synthesis of inorganic materials. (New Delhi: Wiley Eastern Ltd.), (1994)
[5]. K. J. Rao, P D Ramesh, Bull. Mater. Sci. 18:447, (1995)
[6]. G. V. Reddy Gopal, Sheela Kalyana, S V Manorama, Int .J. Inorg. Mater. 2:301, (2000)
[7]. J. Smith, H. P. T. Wijn, N. N. Phillips and G. Eindnoven, Ferrites (Holland) 144, (1959)
[8]. D. A. Sverjensky, Nature 364:776, (2003)
[9]. N. N. Mallikarjuna and A. Venkataraman, Talanta 60:147, (2003)
[10]. N. N. Mallikarjuna, B. Govindraj, L. Arunkumar and A. Venkataraman, J. Therm. Anal. Cal. 71:915 (2003)
[11]. J. C. Mallinson, The foundations of magnetic recording, San Diego: AcademicPress, (1987)
[12]. A.Venkataraman, V. A. Hiremath, S. K. Date and S. M. Kulkarni, Bull. Mater. Sci. 24(6):101 (2001)
[13]. V.Sharabasa, V.Ganachari, R.Bhat. R.Deshpande and A.Venkataraman, 4, 50, (2012)
[14]. H. Vijayanand, L. Arunkumar, N. N. Mallikarjuna and A. Venkataraman, Asian J. Chem.15:79, (2003)
[15]. Monir Doudi, Nasrin Talebian, Biological Forum – An International Journal 8(1): 127-131, (2016).
[16]. Raveendra, R. S., Prashanth, P. A., Hari Krishna, R., Bhagya, N. P., Nagabhushana, B. M., Raja Naika, H., Lingaraju, K., Nagabhushana, H., Daruka Prasad, B., J. Asian Ceram. Soc. 2, 357–365, (2014)
[17]. K. C. Patil, S. T Aruna, T. Mimani, Curr. Opin. Solid State Mater. Sci. 6, 507–512, (2002)
[18]. H.P. Klug, LE Alexander. X-ray Diffraction Procedure, Wiley, New York, (1954)
[19]. Peter Atkins, Julio de Paula, Elements of Physical Chemistry, , 5th edition, Oxford University Press, (2009)
[20]. M. El-Kemary, N. Nagy, I. El-Mehasseb, Mat. Sci .Semicon. Proc. 16, 1747, (2013)
[21]. J. Tauc, F. Abeles, Optical Properties of Solids. North-Holland, Amsterdam, (1970)
[22]. S. Brunauer, P.H. Emmett, E. Teller, J. Am. Chem. Soc. 60, 309–319, (1938)
[23]. R. Gokulakrishnan, S. Ravikumar, J. A. Raj, Asian Pac J Trop Dis., 2, 411-413, (2012)
[24]. G. Geoprincy, N. N. Gandhi, S. Renganathan, Int J Pharm Pharma Sci., 4, 544-548, (2012)
[25]. P. A. Prashanth, R. S. Raveendra, R. H. Krishna, N. P. Bhagya, S. Ananda, B. M. Nagabhushana, K. Lingaraju, H. R. Naika, J. Asian Ceram. Soc. 3, 345, (2015)
[26]. H.U. Simon, A.H. Yehia, F.L. Schaffer, Apoptosis. 5, 415, (2000)
[27]. R.M. Yeaman, N.Y. Yount, Pharmacol. Rev. 55, 27, (2003)
[28]. Y. Shai, Biochim. Biophys. Acta. 1462, 55–70, (1999)
[29]. Zasloff, Michael, Nature. 415, 389-395, (2002)
[30]. A.S. Karakoti, L.L. Hench, S.Seal. JOM. 58, 77–82, (2006)